Available online at www.sciencedirect.com

ScienceDirect

Ceramics International 40 (2014) 4917–4926

CERAMICS INTERNATIONAL

www.elsevier.com/locate/ceramint

Influence of calendering on the properties of paper-derived alumina ceramics

Tobias Schlordt*, Benjamin Dermeik, Veronika Beil[1], Matthias Freihart, Andreas Hofenauer[1], Nahum Travitzky**, Peter Greil

Department of Materials Science (Glass and Ceramics), University of Erlangen-Nuremberg, Martensstr. 5, 91058 Erlangen, Germany

Received 25 June 2013; received in revised form 15 October 2013; accepted 16 October 2013
Available online 25 October 2013

Abstract

The effect of calendering of alumina loaded preceramic papers in a hard nip laboratory calender at various temperatures, line loads and times of nip passes on their green and sintered properties was investigated. The main objective was to achieve a maximum densification, which resulted in a maximum reduction of thickness of 45%, a green density of 80.5% of the theoretical density and a sintered density of 81% of the theoretical density. The ring-on-ring flexural strength of sintered specimen could be increased from 71 ± 11 MPa to 138 ± 33 MPa. The surface roughness of green samples could be diminished to a value for R_a of below 2 μm compared to an R_a of 13.2 μm for an uncalendered paper, whereas the R_a value of the sintered samples was much higher due to the burn-off of the cellulose fibers. Preceramic papers manufactured by the dynamic hand-sheet-forming process exhibit a fiber-orientation which causes anisotropic effects regarding the sintering shrinkage, the surface roughness and Young's modulus.

Keywords: B: Porosity; B: Surfaces; C: Mechanical properties; Preceramic paper

1. Introduction

Commonly available shaping techniques for ceramic structures such as pressing, tape-casting, injection molding or extrusion techniques can be used to create complex light-weight structures. However, these techniques are costly and have a low throughput compared to papermaking machines. Preceramic papers offer a new view on the shaping of ceramic lightweight structures. They exhibit the shapeability and cost-efficiency and production output of common paper while still maintaining the ability to create complex structures with unique properties. Preceramic papers differ considerably from common paper products. Travitzky et al. [1] stated that preceramic papers have to be loaded with at least 75–90 wt% of ceramic powder while common printing and writing papers contain 20–30 wt% of inorganic fillers such as kaolin, alumina or titania. The increased filler content of preceramic papers ensures the successful conversion from preceramic paper to ceramic components, as dense particle-packing is necessary. It has been shown that preceramic papers can be converted into the ceramic state via adapted thermal treatment. Preceramic paper is a fiber enhanced composite material whose properties are significantly defined by the filler that is used. The manufacture of preceramic paper can be performed on commonly used paper machines. The process can be described as a three-stage-process and involves:

a. Preparation of an aqueous suspension containing ceramic powder and pulp at a fixed ratio.
b. Coagulation and flocculation of filler and pulp within the suspension by means of adding organic additives which alter surface charges and interconnect the suspended solids.
c. Formation of paper sheet by dewatering (filtration), followed by wet pressing and drying.

Paper properties such as bending stiffness, porosity and pore size distribution, density and smoothness are heavily influenced by the filler grade, the particle size of the filler and the type of cellulosic fibers that are used.

*Corresponding author. Tel.: +49 91318527548; fax: +49 91318528311.
**Corresponding author. Tel.: +49 91318528775; fax: +49 91318528311.
E-mail addresses: tobias.schlordt@ww.uni-erlangen.de (T. Schlordt), nahum.travitzky@ww.uni-erlangen.de (N. Travitzky).
[1]Papiertechnische Stiftung, Heßstraße 134, 80797 München, Germany.

0272-8842/$ - see front matter © 2013 Elsevier Ltd and Techna Group S.r.l. All rights reserved.
http://dx.doi.org/10.1016/j.ceramint.2013.10.080

Calendering is a common procedure to affect density, surface roughness, gloss and stiffness/strength of a paper. There are several techniques how paper and paperboard can be calendered. The principle of each technique is that paper or paperboard is fed through a couple of steel rolls (nip), of which one roll is commonly coated with compressed cotton or paper to achieve a larger nip area and better pressure distribution, while the other (the heated thermoroll) is polished to achieve the smoothness of the paper. Another technique, so called softcalendering, involves a polymer coating of the unheated roll. This kind of calender has an increased nip area and higher dwell times due to the low elastic modulus of the polymer coating and achieves a more homogeneous compression, whereas the thickness of the paper cannot be controlled as accurately as in a hard nip calender. The nip pressures generally decrease from hard nip to soft nip calendering. The hard nip calenders used in paper fabrication typically have a nip length of 1–5 mm, whereas soft nip systems reach up to 20 mm. Thus dwell times are considerably higher and the nip pressure is decreased [2,3]. When using a softcalender, Groshek reported a nonproportional nip load to nip pressure correlation caused by the resilient nip. An increase of nip pressure by a factor of 2.5 when increasing the nip load by a factor of 5 (88–439 N/mm) was determined [4].Calendering often involves softening of the pulp component of the paper by temperatures exceeding the glass transition temperature of the amorphous content. Salmen [5] reports the temperature of softening (interpreted as glass-transition of the cellulose–hemicellulose–water system) to be strongly dependent on the pulp moisture. Blechschmidt et al. [6] mention a major contribution of the nature of the pulp to the glass transition temperature. They also state that the "extent of softening" becomes more emphasized with higher moisture content. Furthermore, the glass transition of the pulp does not occur at a single distinct temperature, but is rather a superposition of the glass transition temperatures of its constituents. Although Dwan [7] defines the glass transition temperature of cellulose to be at 240 °C and the one of hemicellulose to be at 190 °C, there is a broad softening region of the pulp at a certain temperature range as the natural material differs greatly in chemical composition. Haslach [8] reports 40–60% crystalline regions to be common within pulp for papermaking. A study by Paes et al. [9] investigated the glass transition of ball milled, thus mostly amorphous cellulose using thermal and mechanical methods at various moistures. They found dynamical–mechanical methods (DMA) superior to DSC and obtained T_g values from 320 to 380 K from 10% to 19% humidity (dry weight base). Additionally they stated, that upon wetting and heating, recrystallization of the amorphous content commonly occurs. The corresponding recrystallization temperatures are 15–20 K above T_g. According to Fornué et al. [10], cellulose fibers are bonded by a combination of mechanical interlocking, intermolecular diffusion of molecular chains between cellulosic surfaces and chemical interaction and attraction. The authors described hemicelluloses as dry agents adhering onto the cellulose fiber by hydrogen bonds and electrostatic interactions. Moisture contents of above 10% within the paper cause the separation of microfibrils and the breaking of hydrogen bonds. Browne et al. [11] modeled the calendering process by using a nonlinear viscoelastic Burgers four element model, describing paper behavior being composed of a direct elastic response (spring), serially coupled with a viscous response (dashpot) and a restrained elastic response (parallel dashpot and spring), based on observations of calendered newsprint paper which shows relaxation phenomena (expansion) after leaving the nip. With increasing strain the paper becomes more rigid as the cellulose microfibrils collapse and become increasingly incompressible. Due to the variety of wall thicknesses of the fibrils, compression resistance does not increase instantaneously. The compression of paper while calendering was suggested to proceed in a three stage process. First, surface defects and porosity are eliminated whereafter buckling of the fibers occurs due to their hollow nature. In the last step, further compression can only be achieved by crushing of the fibers [12]. A pressure onto a random fiber network inducing bulging at the fiber contact points prior to further collapse was observed by Lundquist et al. [13]. Enomae et al. [14] investigated the effect of calendering conditions (softcalendering vs. supercalendering, temperature, speed, line load) on wood containing and wood free paper (thickness of 56–101 μm) under industrial conditions. Smoothness and thickness reduction were investigated. They concluded that high temperatures, high line loads and low speeds are beneficial for densification and smoothness. A higher line load results in a larger nip area and thus a better heat transfer, whereas the actual pressure in the nip does not correlate linearly with the line load. The achieved roughness values (R_a) were ~1 μm and softcalendering (177 °C, 2 nips) showed to be modestly superior to supercalendering (90 °C, 10 nips), while its efficiency was much higher. Softcalendering showed to improve smoothness and gloss at a low bulk reduction, which is attributed to the distinct temperature gradient between surface and bulk. This is achieved by a combination of the very hot rolls and a good surface contact and thus a good heat transfer [15]. A study by Steffner et al. investigated calendering (using single hard and soft nips) of a woodfree paper filled with 24 wt% $CaCO_3$. They found a hard nip to be beneficial to even out the larger defects of the paper and achieve a narrower distribution of thickness, while softcalendering could better compress the thinner spots of the paper [16].

Kluthe et al. [17] evaluated calendering parameters of preceramic papers on density and flexural strength, while their calendering parameters were limited to 100 °C and 250 N/mm line load. All preceramic papers passed the hard nip (identical calender as used in this work) once and showed a considerable increase in sintered flexural strength, green and sintered density. The authors showed that during calendering of preceramic paper, the surface densification of the preceramic paper is also more pronounced than the densification of the core region, despite the low calendering speed of 0.5 m/min. Kluthe and Kollenberg also investigated the surface roughness of preceramic papers depending on the calendering parameters and found calendering as beneficial for reducing the surface roughness, however, no information about roughness of the sintered ceramic and anisotropy due to the use of oriented fibers was provided [18]. The present work takes further insight into surface roughness and mechanical properties at enhanced calendering conditions. Furthermore the influence

of oriented fibers from the applied papermaking-process on Young's modulus and surface roughness is investigated.

2. Materials and methods

2.1. Paper formation

Preceramic papers containing 85 wt% bimodal Al_2O_3 powder (NABALOX 625-31, Nabaltec AG, Schwandorf, Germany) with a primary grain sizes of 0.5 and 2 µm, a specific surface area of 4 m^2/g, 11.72 wt% pulp (Aracruz (SR 31), Fibria (Europe) S.A., Nyon, Switzerland/São Paulo, Brazil) with an average fiber length of 0.74 mm, a width of 12.2 µm and a thickness of 2.3 µm, 3.28 wt% retention agent (Percol 540, BASF AG, Ludwigshafen, Germany) and binder (Nychem 1562 × 117, Emerald Performance Materials LLC, Cuyahoga Falls, USA) at grammages of 950 g/m^2 (0.65 ± 0.032 mm thickness) was prepared by using a dynamic hand-sheet former (Valmet Fibertech AB, Sundsbruk, Sweden), see Fig. 1. The flow rate of the hand sheet former pump was set to 1425 ml/min, while the wire speed was set to 1000 rpm, the maximum speed of the device. Tap water (9.8 °C, pH 7.6, 2.9 mmol/l alkaline earth concentration) was used for the process of sheet formation.

A parameter characteristic for the fiber orientation is the ratio of the tensile stiffness along MD in relation to the tensile stiffness along CD, described with TSI-MD/CD. This procedure resulted in the manufactured paper having a TSI-MD/CD value of 1.43, whereas typical TSI-MD/CD values of common papers are much higher according to Lindblad and Fürst [19] and Loewen and Foulger [20], implying a more distinct fiber orientation. However, low TSI-MD/CD values, compared to typical newsprint paper (3.5–4.8), copy paper (2.0–2.5) or label paper (1.8–2.2) are commonly associated with good dimensional stability as stated by Loewen and Foulger [20].

2.2. Sample preparation, selection and nomenclature

Calendered sheets (170 × 280 mm^2) were cut in half perpendicularly to MD. A 10 mm wide margin of the sheet was removed to ensure non-lacerated paper edges. The resulting sheet was divided into 15 equally sized square samples (three rows with five samples on each), from which circular samples were punched out for the measurements of the vertical shrinkage and flexural strength by the ring-on-ring test (Fig. 2). Six samples (two rows with three samples on each) were cut out for measurement of the lateral shrinkage, the surface roughness and Young's modulus. The sample size was 30 × 50 mm^2.

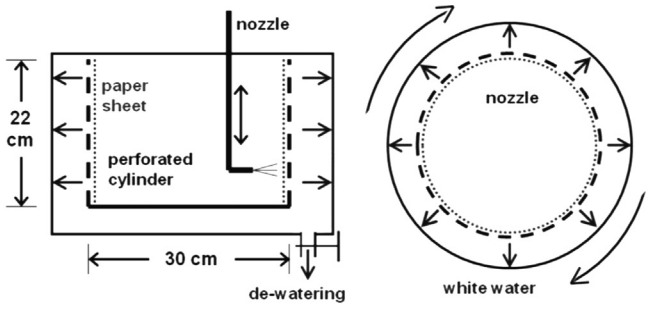

Fig. 1. Schematic drawing of the dynamic hand sheet former.

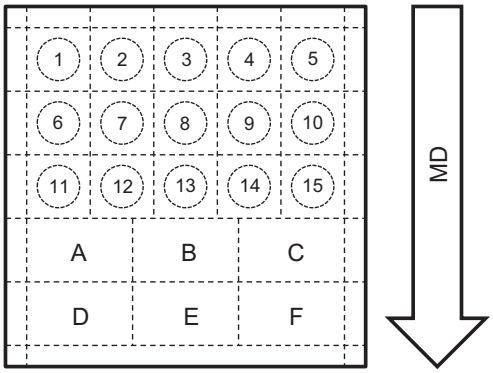

Fig. 2. Location of the cut out samples within a calendered sheet.

2.3. Calendering

Preceramic papers were calendered by a single nip laboratory calender with separately heatable hardened steel rolls (CA5/250-150-20, Sumet Systems GmbH, Denklingen, Germany) of a diameter of 150 mm. Three temperature values (100, 150 and 200 °C) and three line load values (14.7, 73.5 and 368 N/mm) were applied for calendering. Each combination was calendered once and twice. The samples had a water content of about 1.2 ± 0.13 wt% shortly before calendering corresponding to a pulp moisture of around 8% which could be determined with a thermobalance (MLS 50-3, Kern & Sohn GmbH, Balingen-Frommern, Germany) applying 105 °C. The calendering speed was kept constant at 0.5 m/min.

2.4. Surface roughness measurements

The surface roughness of the papers was determined using a laser scanning surface tester (Laser Scanning Microscope, UBM Messtechnik GmbH, Ettlingen, Germany). Three lines of 20 mm in length were scanned in the middle of the sheet in cross-machine direction (CD) and three lines of the same length were scanned in MD; the distance between the parallel lines was 10 mm. The evaluation of the average surface roughness was performed according to the standard DIN EN ISO 4287:2010. The scan was performed with 1000 measurements per mm.

2.5. Sintering analysis and shrinkage determination

Flat sheets of preceramic papers were sintered using an electrically heated furnace while being encapsulated in kiln furniture. First, the samples were heated up 250 °C in 480 min with a subsequent dwell time of 120 min. Next, the samples were heated up from 250 to 500 °C in 360 min with a subsequent dwell time of 120 min, followed by a heating-up from 500 to 1700 °C in 840 min and a dwell time of 240 min. Finally, a sequence of cooling steps took place: from 1700 to 1400 °C in 210 min, from 1400 to 900 °C in 240 min, from 900 to 500 °C in 150 min, from 500 to 300 °C in 60 min and finally from 300 °C to room temperature in 75 min. The lateral sintering shrinkage in

the *x*–y plane was obtained optically by comparing scanned (resolution 42 μm) green samples with sintered samples. The vertical sintering shrinkage was determined by relating the thicknesses of the samples, which were measured using a tapered micrometer gauge. Measurements were performed at five different locations of each circular shaped sample.

2.6. Young's modulus measurements

Young's modulus of sintered samples was measured on samples A–F by ultrasonic testing using a USD 10 apparatus (GE Sensing & Inspection Technologies GmbH, Hürth, Germany) according to the standard EN 843-2:2006. The porosity dependent Poisson numbers for calculation of *E* were taken from a study of Asmani et al. who also investigated porous alumina with ultrasonic methods [21]. An attempt to determine the Young's modulus values by the standard EN ISO 12680-1:2007, where it is calculated from the sample dimensions, the sample weight and the resonance frequency, lead to significantly higher standard deviations.

2.7. Flexural strength measurements

Flexural strength was measured by means of the ring-on-ring method according to the standard DIN 51105:2010-08, which requires the maximum stress to be applied to a circular area. This requirement is crucial to measure independently from inhomogenities of the preceramic papers on a millimeter scale, which could be confirmed by light transmission images (Fig. 10). The flexural strength was determined on a mechanical testing machine (Instron Model 4204, Instron Deutschland GmbH, Pfungstadt, Germany). The loading rate of the instrument stage was at 5 mm/min. The ring diameters were 12 mm (top) and 16 mm (bottom). The thickness values for 15 samples of each calender setup were determined by a tapered micrometer gauge at five points of each sample.

2.8. Optical investigations

Sample homogeneity was analyzed using a flatbed scanner (resolution 42 μm) revealing the light transmission distribution within sintered samples. The fiber and surface topography was furthermore investigated with scanning electron microscope (Quanta 200, FEI Company, Hillsboro, USA) on green and sintered samples.

2.9. Thermal measurements

Thermomechanical measurements (TMA) were carried out on 3×3 mm^2 pulp fiber samples pressed to a density of 0.96 g/cm^3 and analyzed using a TMA-60H apparatus (Shimadzu EUROPA GmbH, Duisburg, Germany). A force of 0.1 N was applied up to 200 °C while heating up was performed at a rate of 10 K/min. A thermogravimetric analysis (TGA) of the uncalendered preceramic paper was conducted via a thermal analyzer (STA 429, Netzsch Gerätebau GmbH, Selb, Germany).

3. Results and discussion

The samples are referred to according to the following nomenclature: *Calendering temperature – line load – number of passes through the nip*. For example, the combination 100-368-2 stands for a calendering temperature of 100 °C, a line load of 368 N/mm and two passes through the nip of the calender.

3.1. Thermal analysis

The TMA measurement of the pulp fibers reveals a softening onset at about 50 °C while the maximum compression rate is reached at about 80 °C (Fig. 3). The flattening of the curve above 130 °C in the TMA measurement appears due to the fact, that the sample approaches its maximum compression at this temperature and thus thermal expansion dominates over yielding under the applied load.

The TGA of the preceramic paper reveals a slight loss of paper moisture below 100 °C and decomposition of the pulp above 200 °C (Fig. 4). Therefore, the temperature of 200 °C was set as limit for the applied calendering temperatures.

3.2. Density measurements

Thickness reduction and densification of the preceramic paper mainly correlate with an increasing line load, which is observable at all of the calendering temperatures (Fig. 5).

A second pass of the nip increases the thickness reduction regardless of the other conditions. The obtained sintered density of the paper-derived ceramics correlates with the green density of the preceramic paper. Thus, calendering represents an effective way to tailor the density of paper-derived ceramics. A systematical effect of temperature on the thickness reduction could only be observed at the highest of the applied line loads. To explain this effect, we first approximate the time necessary for heat transfer. Therefore, the approximate nip length, describing the

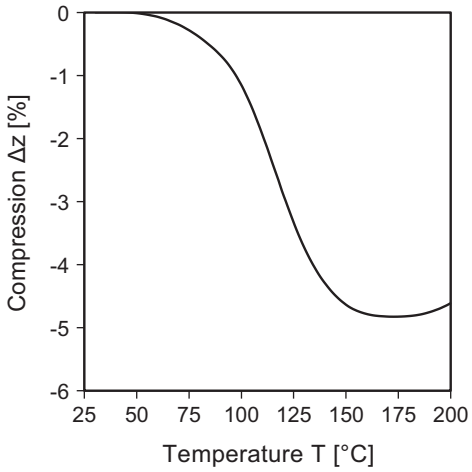

Fig. 3. TMA of the pulp component.

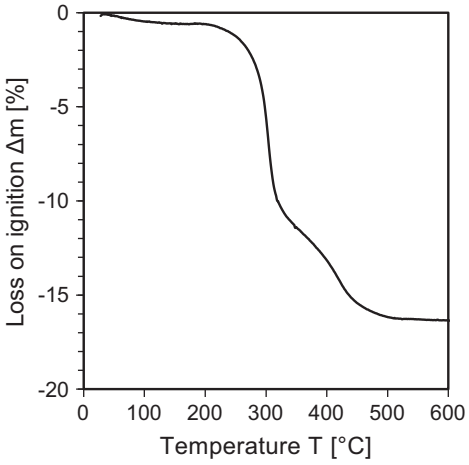

Fig. 4. TGA of the preceramic paper.

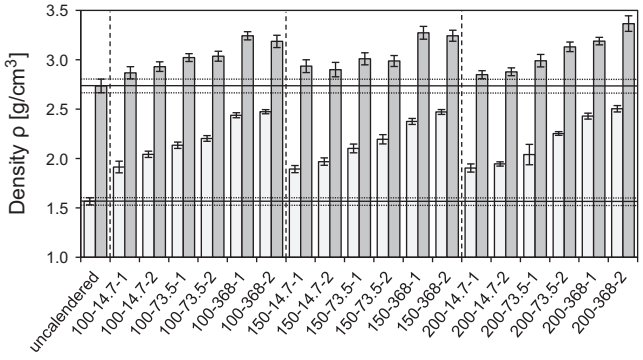

Fig. 5. The green density vs. the sintered density for different calendering conditions.

contact length between the paper and two calender rolls, l, with

$$l \approx \sqrt{R^2 - \left(R - \frac{(d_1 - d_2)}{2}\right)^2} \tag{1}$$

can be calculated with R being the roll radius, d_1 denoting the paper thickness before the nip and d_2 denoting the paper thickness after the nip ($l \approx 4.2$ mm at maximum thickness reduction vs. ≈ 2.9 mm at minimum thickness reduction). For calculating the nip length it is assumed that no relaxation of paper takes place after calendering. Thus, the nip area, A_{nip}, can be calculated as shown in Eq. (2). The quantities contained in this equation are also shown in Fig. 6.

$$A_{nip} = 2sw = 2R\frac{\theta}{2}w = 2R\cos^{-1}\left(1 - \frac{(d_1 - d_2)}{2R}\right)w \tag{2}$$

where s is the segment of one roll in contact to the paper being calendered, thus the contact length between one roll and the paper, w is the width of the paper sheet and θ is the central angle of a segment double the size of the segment s.

The maximum temperature generated in the bulk of the calendered preceramic paper can be calculated by applying the transient-state conduction Eq. (3) for the heat transfer.

$$\frac{\partial T}{\partial z^2} = \frac{\varphi c_P}{k_P}\frac{\partial T}{\partial t} \tag{3}$$

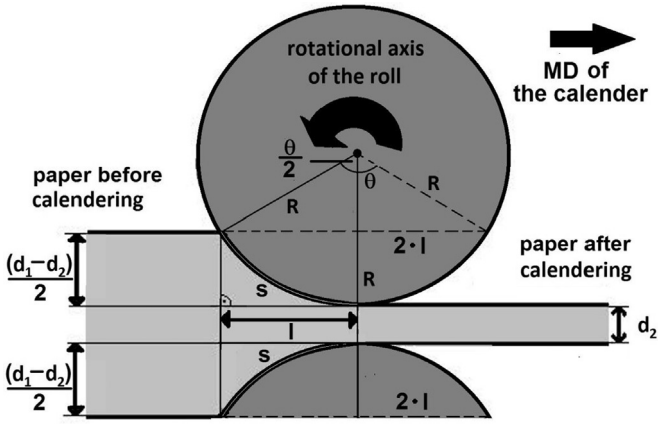

Fig. 6. A schematic cross-section view of a preceramic paper being calendered by the two calender rolls.

Within the work of Kerekes [22] the transient-state equation has been solved for the boundary conditions occurring at a heat transfer from the hot calender rolls to an processed sheet of paper. Thereby, all three physical processes of heat transfer had been considered: conduction, convection and radiation. In order to simplify the complicated equation system deducted by Kerekes, the first approximation can made by only considering heat conduction, under the assumption of the paper to be in an intimate contact with the calender rolls. Further assumptions to be made are the occurrence of an uniform deformation of the paper in the nip and the initial temperature of the paper being equal to room temperature. After the application of a Taylor series, Eq. (4) can be derived, including the exponent k_C. Thereby, the last term is negligible, if the condition $k_C > 0.05$ is fulfilled.

$$\frac{T(z)}{T_R} = \left|1 - \frac{2e^{-k_C}\cos\left(\sqrt{Bi_s}(1-(z/d_1))\right)}{(2+Bi_s)\cos\left(\sqrt{Bi_s}\right)} - \sum_{n=2}^{\infty}\frac{(-1)^{n+1}2Bi_s e^{-(\pi^2(n-1)^2 k_C)/Bi_S}}{(Bi_S{}^2 + Bi_S + (n-1)^2\pi^2)}\cos\left(\frac{(n-1)\pi(d_1 - z)}{d_1}\right)\right|$$

with

$$k_C = \frac{\lambda_P Bi_S 2l}{W c_P d_1 V} \quad \text{and} \quad Bi_s = \frac{c_P h_S d_1}{\lambda_P} \tag{4}$$

Thus, the ratio between the temperature $T(z)$, at the position z, and the roll temperature, T_R, can be calculated in dependence of several physical quantities. The specific heat capacity of the paper, c_P, the Biot number, Bi_S, depending on the contact resistance between the preceramic paper and each of the two rolls, h_S, and the thermal conductivity of the paper, λ_P, are as well important as the average surface density of the paper, W (also denoted as grammage) and the calendering velocity, V. The Biot number, the heat capacity and the heat conductivity of the preceramic paper are depending on the single values of the pulp and the filler, as well as on the weight ratio pulp and the filler. As the preceramic paper was filled with 85 wt% of alumina, these quantities can be calculated by Eqs. (5) and (6). Table 1 displays all the single values of the three quantities, which are cited from the literature.

$$c_P = 0.85c_{P(Al_2O_3)} + 0.15c_{P(pulp)} \tag{5}$$

Table 1
The Biot numbers, the heat capacities and the thermal conductivities of alumina and pulp.

Physical quantity	Alumina	Pulp
Biot number, Bi_S (dimensionless)	0.035, Taken from [23]	0.5, Taken from [22]
Heat capacity, c_P (J/(kg K))	765, Taken from [24]	1500, Taken from [25]
Heat conductivity, λ_P (W/(m K))	1, Taken from [26]	0.01, Taken from [27]

$$h_S = 0.85h_{s(Al_2O_3)} + 0.15h_{S(pulp)} \quad (6)$$

By applying Eqs. (5) and (6), the specific heat capacity of the paper, c_P, becomes 875.25 J/(kg K) and the Biot number becomes 0.105. Due to the thermal conductivity being being influenced by the paper porosity, a value of ~1 W/(m K) at a porosity of 57.5% (the highest measured value before calendering) [26] was used for the alumina. The thermal conductivity of the pulp was modeled in the work of Faessel et al. [27], whereby a network of randomly distributed and bent cellulose fibers was considered. The resulting heat conductivity of the cellulose fiber network varied between 0.01 and 0.07 W/(m K) and thus can be considered as negligible for our calculations. From Eq. (4) the temperature inside the bulk of the paper, at the position $z=d_1/2$, was calculated to reach ~99%, corresponding to an almost complete heat transfer at calendering parameters with the lowest nip area and the lowest compression (200-14.7-1). Thus as an almost complete heat transfer can be safely postulated in all of our experiments, considerable yielding could be measured at the utilized temperatures (Fig. 3) and the preceramic paper exhibits open porosity, one would rather expect a plastic than an elastic behavior of the preceramic paper while calendering. For the mechanical behavior of the pulp in the vicinity of T_g is highly dependent on temperature and a shift from elastic to viscous behavior takes place, the increased thickness reduction due to temperature becomes measureable at the maximum line load. Furthermore, elastically stored energy can dissipate through viscous deformation at high temperatures and thus expansion after the nip may be reduced.

3.3. Sintering shrinkage analysis

The lateral shrinkage could be reduced from 18% to 12%, while the vertical shrinkage (ZD) could be reduced from 27.5% to 14.4% (Fig. 7a–c). It would have been expected, that the lateral shrinkage in MD would significantly differ from the lateral shrinkage in CD due to the anisotropically oriented fibers of the preceramic paper sheets. The difference between the lateral shrinkage values, however, is below 1%. It is likely that a more pronounced anisotropy would occur at faster wire speeds, leading to more pronounced differences between the lateral shrinkage values. It was observed that upon increasing thickness reduction by calendering the sintering shrinkage in ZD is reduced to a greater extent than in lateral direction. As interparticle and pulp templated voids adapt a flat shape during calendering, they are assumed to counteract the sintering shrinkage in ZD as they strive for a spherical/circular shape while sintering.

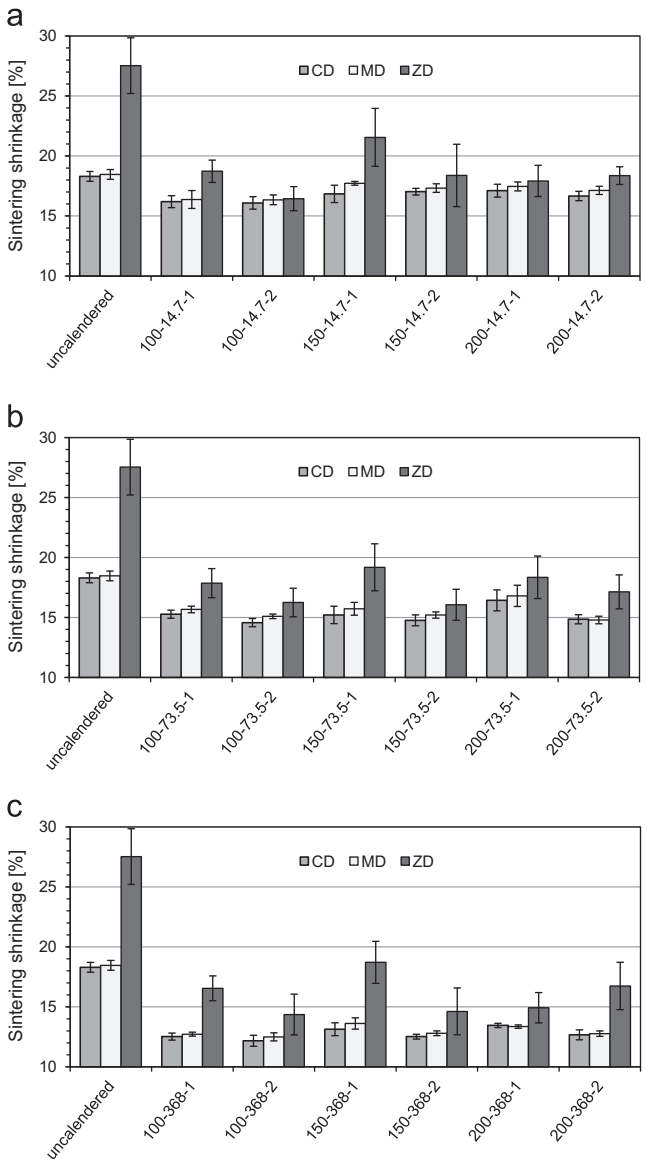

Fig. 7. (a) Sintering shrinkage of samples calendered at a line load of 14.7 N/mm, (b) Sintering shrinkage of samples calendered at a line load of 73.5 N/mm and (c) Sintering shrinkage of samples calendered at a line load of 368 N/mm.

3.4. Surface and microstructural analysis

The average surface roughness of preceramic paper and the corresponding sintered samples is diminished considerably by calendering (Fig. 8a). A clear difference between the average surface roughness in MD and the average surface roughness in CD can be detected for all of the paper samples (Fig. 8a and b).

Against intuitive expectation, in most of the cases the average surface roughness of paper sheets being calendered twice is marginally increased, instead of decreased, in comparison to the same paper sheets being calendered for a single time. However, the average surface roughness of the paper sheets mainly decrease dependent on the applied line load, reducing the R_a value below 8 µm. In contrast, the uncalendered paper sheets display R_a values in the range of 9–13 µm. A similar relationship between the average surface roughness and the applied line load during calendering can be observed for the paper-derived ceramics (Fig. 8b). Also, the average surface roughness of the ceramics derived from all of the calendered paper sheets is below 8 µm.

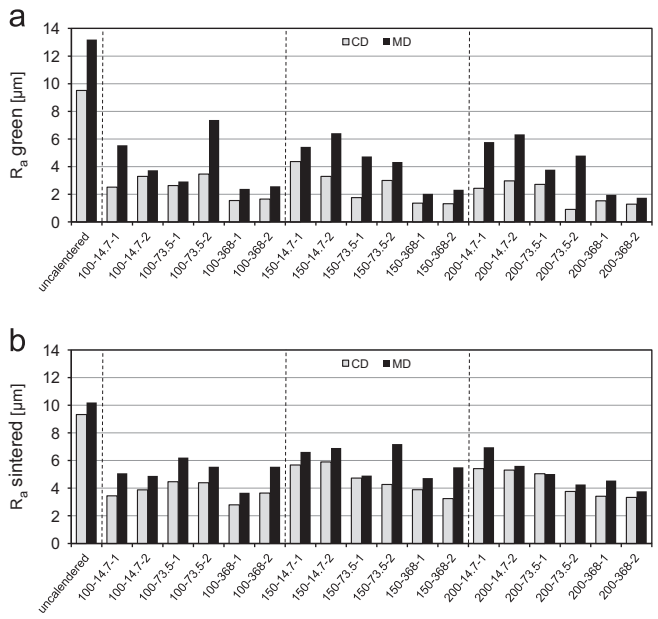

Fig. 8. (a) Average surface roughness of preceramic papers calendered at different calendering parameters and (b) Average surface roughness of sintered paper-derived ceramics calendered at different calendering parameters.

The pulp fibers tend to orientate in parallel to the surface of the calendered paper as well as of the uncalendered preceramic paper (Fig. 9a and c).

This is especially beneficial for lowering the average surface roughness of the sintered ceramic. The orientation of the pulp fibers parallel to the paper surface is caused by their oval cross section and their flat surface. The maximum depth of pits left from burned off pulp fibers is the main contribution to the average surface roughness of the sintered ceramic. Therefore, the average surface roughness is limited by the pulp fiber geometry (Fig. 9b and d). Surface profiles of the sintered ceramic showed considerable surface features within the range of 10 µm which correspond to the fiber width. Furthermore, features within the size of 1 mm are visible, which correspond to the wavy surface generated by using the dynamic hand sheet former at the given paper grammages (Fig. 10).

The higher values for R_a in MD are most likely to be caused by the wavy surface of the paper. This relation between the different R_a values persists also for the sintered ceramic.

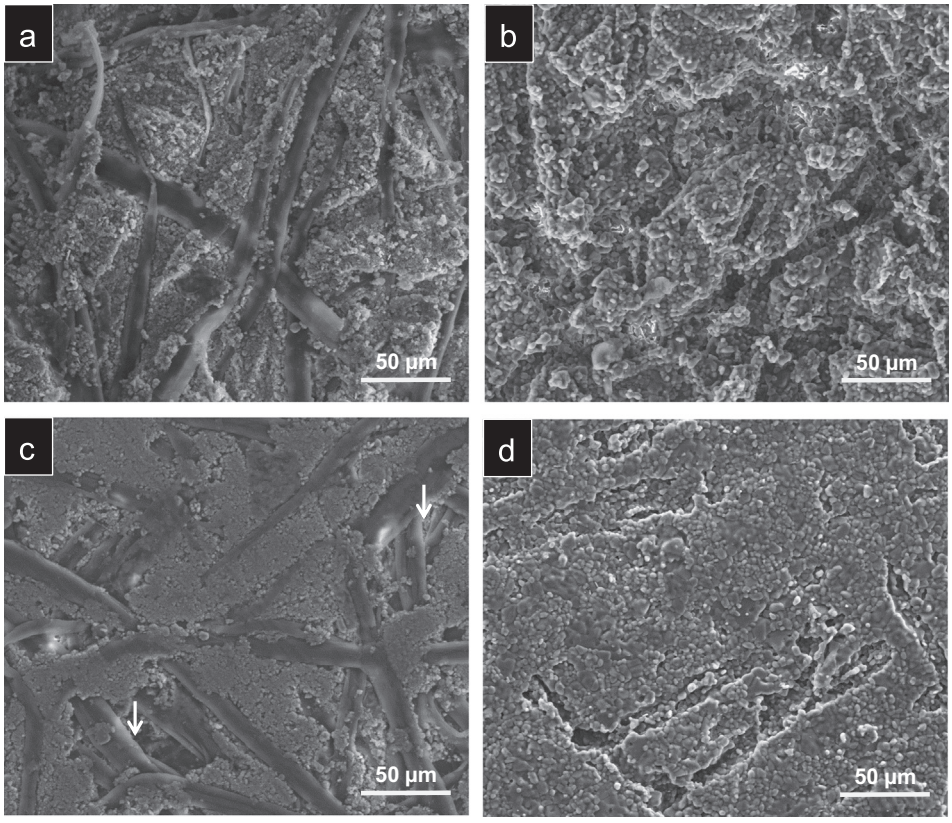

Fig. 9. SEM micrographs of uncalendered preceramic paper (a) and paper calendered at 200 °C, 368 N/mm in one pass (c), as well as the ceramics derived from the uncalendered paper (b) and the calendered paper (d). The white arrows in (c) point out areas crucial for the surface roughness, where cellulose fibers are not surrounded with alumina particles.

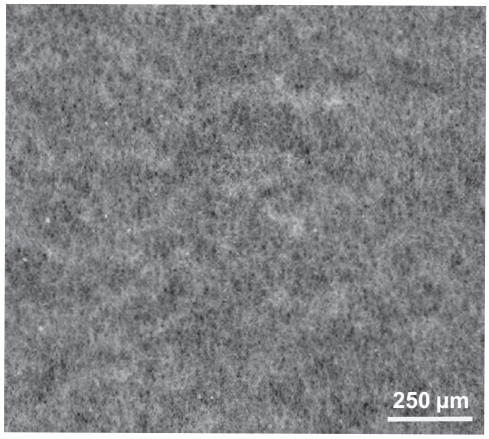

Fig. 10. Light transmission image of a sintered paper-derived ceramic (200-368-2), where MD is along the vertical direction.

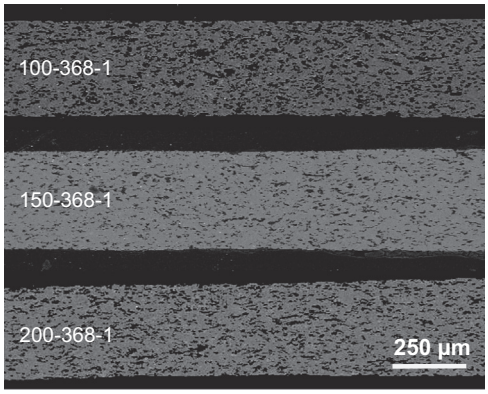

Fig. 11. SEM micrograph of sintered samples cut perpendicularly to MD.

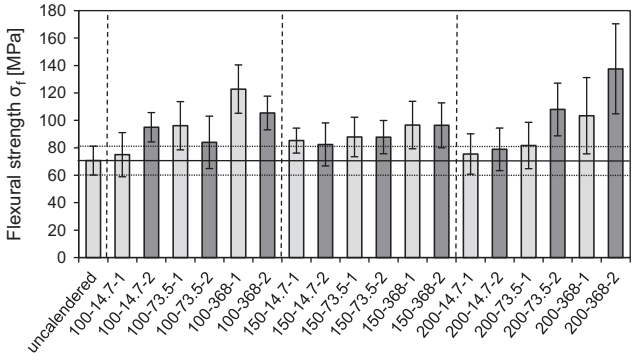

Fig. 12. Flexural strength of the paper derived ceramics for various calendering conditions.

The average surface roughness of the calendered green samples is also governed by a lack of particles circularly around the fibers (Fig. 9c). The roughness of the steel rolls plays a minor role for the overall surface roughness, but is visible on SEM micrographs (Fig. 9c, diagonal grooves). The roughening accompanied by multiple passes of the nip may be caused by nonuniform roll-contact, small nip area and inhomogeneous drag forces, when precalendered paper is used. To overcome these detrimental effects, a softcalender may be an improvement, as a larger nip area with enhanced and more homogeneously distributed friction in comparison to the hard nip calender can be generated. The paper composition and the calendering conditions applied in this work facilitate a compaction of the whole bulk (Fig. 11), whereas Kluthe et al. observed a pronounced density gradient within their preceramic papers at the highest line loads and temperatures (100 °C, 250 N/mm) [17]. Due to the fact that they used tubular pulp fibers, fiber collapses were observed in the vicinity of the surface. The flat and compact pulp fibers used in our work are most likely responsible for a better pressure transmission while calendering, thus no evident density gradient in ZD was observed after the first nip-pass at similar line loads, regardless of temperature.

3.5. Mechanical properties

The mechanical strength of the paper-derived ceramic is increased considerably by calendering reaching maximum values of 138 ± 33 MPa which is about the double strength of uncalendered paper-derived-ceramic (Fig. 12). The rather poor consistency of these values may be mainly due to the wavy surface of the preceramic papers, which during hard nip calendering undergo only slight compression at their depths, from which weak spots remain. Also here a softcalender would possibly achieve a better compression of the areas of decreased bulk and lead to higher flexural strengths and reliabilities.

Reasonable results were obtained for Young's modulus using both, the resonance and the ultrasonic transmission method. However, the ultrasonic transmission method proved to be more accurate for the kind of material examined. The results show a clear correlation between Young's modulus and the sintered density (Fig. 13). Due to the fiber orientation, Young's modulus displays a dependence on the sintered density of the sample, ρ_s, and the direction of the ultrasound transmission. Exponential fitted data within the investigated range resulted in

$$E_{MD} = 9.6981e^{0.9973\rho_s} \quad (7)$$

for MD and

$$E_{CD} = 9.0385e^{0.9905\rho_s} \quad (8)$$

for CD.

Models for calculating the elastic modulus based on tubular pore geometries [28] and such involving an orientation [29] mostly result in too high E values and are not applicable to paper-derived ceramics. Roughly comparable values for a theoretical Young's modulus can be obtained, when either spherical, cubic or cross pore models [28], or a complete alignment of tubular (aspect ratio k is considered as infinite) pores in CD is applied [29]. Generally, the drop of elastic modulus with increasing porosity appears to be somewhat more pronounced than expected. Compared to an alumina ceramic with tubular porosity formed by burnout of highly aligned carbon fibers ($d = 14$ µm, $l = 600$ µm) [30], Young's modulus is still expected to be significantly lower at the given volumetric fraction of the porosity. Yet, another study by Asmani et al. [21], who also used ultrasonic impulse transmission to measure the elastic modulus of partly sintered and thus porous

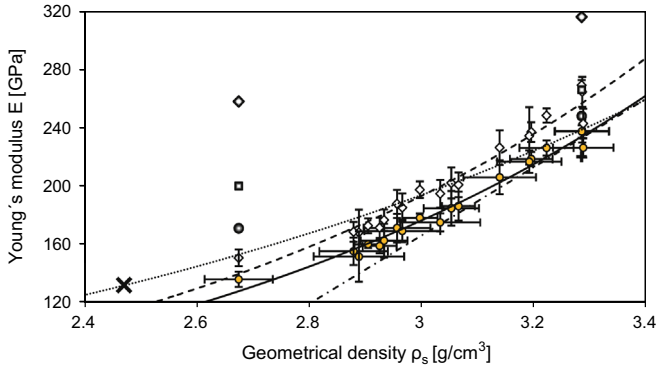

Fig. 13. Plot of Young's modulus vs. the sintered density. The hollow markers and the dashed line represent measured data for MD, the filled markers and the continuous line represent CD. Error bars for density only displayed for CD (values are identical for MD). The dotted upper line indicates model data by Andersson (fibers completely oriented along CD, aspect ratio of the fibers is infinite) [29]. The alternating dashed and dotted lower line indicates the measured values of Asmani et al. [21]. The cross at the left side represents the highly aligned porosity ceramic by Isobe et al. [30]. Big, gradually filled symbols represent model data by Herakovich and Baxter [28], where diamonds represent tubular pores, squares cubic pores, circles spherical pores and crosses cross shaped pores.

alumina of open porosity showed results comparable to CD, whilst the MD values of the paper derived ceramics still are higher.

4. Conclusion

Calendering showed to be a simple and suitable method to adapt and improve the properties of preceramic papers and the ceramics derived from these papers. Density and surface roughness can be altered within an extensive range, while the surface roughness of sintered samples is mainly limited by the pulp fiber dimensions and by buckling effects caused by the papermaking process. Anisotropy caused by the papermaking-process was observed among sintering shrinkage, green and sintered roughness as well as among Young's modulus of the derived ceramic. The mechanical strength was significantly improved by hard nip calendering, while softcalendering might even lead to higher values of mechanical strength and reliability, due to a more homogeneous compression. The use of flat pulp fibers is suggested to give rise to an improved pressure transmission, making density gradients avoidable. Furthermore the ultrasound transmission method showed to be a precise method to measure Young's modulus. Young's modulus of paper derived ceramics exhibits a somewhat unexpected correlation with porosity revealed by a pronounced decline with increasing porosity, while a significant anisotropy between MD and CD could be observed.

Acknowledgments

The authors gratefully thank for funding based on the AIF Project IGF 16485N and DFG Project TR-250/4-1. Mr. Jan Kupfer from Nabaltec AG is acknowledged for the kind supply of ceramic powders. Further thanks go to Mr. Norbert Müller from LAPP Insulators Alumina for organization and set up of the firing process.

References

[1] N. Travitzky, H. Windsheimer, T. Fey, P. Greil, Preceramic paper-derived ceramics, J. Am. Ceram. Soc. 91 (2008) 3477–3492.
[2] P. Svenska, Glättung von Papier und Karton – Heutiger Stand der Technik, Wochenbl. Papierfabr. 130 (2002) 1590–1593 (in German).
[3] A. Todorović, T. Hämäläinen, Proceedings of the Shoe Nip Calender Possibilities for Board and Paper, Tappi Spring Technical Conference, 2003.
[4] J.M. Groshek, Finishing alternative for offset LWC, Tappi 77 (1994) 105–110.
[5] L.N. Salmen, E.L. Back, Moisture-dependent thermal softening of paper, evaluated by its elastic modulus, Tappi 63 (1980) 117–120.
[6] J. Blechschmidt, P. Engert, M. Stephan, The glass transition of wood from the viewpoint of mechanical pulping, Wood Sci.Technol. 20 (1986) 263–272.
[7] A. Dwan, Paper complexity and the interpretation of conservation research, J. Am. Inst. Conserv. 26 (1987) 1–17.
[8] H.W. Haslach, The moisture and rate-dependent mechanical properties of paper: a review, Mech. Time Dep. Mater. 4 (2000) 169–210.
[9] S.S. Paes, S. Shaomin, W. MacNaughtan, R. Ibbett, J. Ganster, T. J. Foster, J.R. Mitchell, The glass transition and crystallization of ball-milled cellulose, Cellulose 17 (2010) 693–709.
[10] E.D. Fornué, G.G. Allan, H.J.C. Quiñones, G.T. González, J.T. Saucedo, Fundamental aspects of adhesion between cellulose surfaces in contact – a review, O Papel 72 (2010) 85–90.
[11] T.C. Browne, R.H. Crotogino, W.J.M. Douglas, Viscoelastic modeling of paper in a calender nip, J. Pulp Pap. Sci. 22 (1996) J170–J173.
[12] P. Rättö, Description and analysis of paper deformation in a calendar nip – effects of high roll temperatures and thickness variations, Nord. Pulp Pap. Res. J. 17 (2002) 130–138.
[13] L. Lundquist, F. Willi, Y. Leterrier, J.-A.E. Månson, Compression behavior of pulp fiber networks, Polym. Eng. Sci. 44 (2004) 45–55.
[14] T. Enomae, T. Huang, P. LePoutre, Softcalendering: effect of temperature, pressure and speed on sheet properties, Nord. Pulp Pap. Res. J. 12 (1997) 169–175.
[15] R.J. Kerekes, I.T. Pye, Pulp Pap. Can. 75 (1974) T359.
[16] O. Steffner, T. Nylund, M. Rigdahl, Influence of the calendering conditions on the structure and the properties of woodfree paper – a comparison between soft nip and hard nip calendering, Nord. Pulp Pap. Res. J. 13 (1998) 68–75.
[17] C. Kluthe, B. Dermeik, W. Kollenberg, P. Greil, N. Travitzky, Microstructure and properties of paper-derived porous Al_2O_3 substrates, J. Ceram. Sci. Technol. 3 (2012) 111–118.
[18] C. Kluthe, W. Kollenberg, Paper-derived stoneware ceramics: improvement of properties by calendaring and evaluation of pyroplastic deformation behavior, Mater.-wiss. Werkstofftechn. 44 (2013) 1–5.
[19] G. Lindblad, T. Fürst, The Ultrasonic Measuring Technology on Paper and Board, Lorentzen & Wettre, Kista, 2001.
[20] S. Loewen, M. Foulger, Tensile Stiffness Properties: TSI, TSO and Fibre Orientation: an Introduction, 2002. ⟨http://www.pulpandpapercanada.com/news/tensile-stiffness-properties-tso-and-fibre-orientation-an-introduction/1000185068/⟩ (accessed 05.28.13).
[21] M. Asmani, C. Kermel, A. Leriche, M. Ourak, Influence of porosity on Young's modulus and Poisson's ratio in alumina ceramics, J. Eur. Ceram. Soc. 21 (2001) 1081–1086.
[22] R.J. Kerekes, Heat transfer in calendering, in: Proceedings of the Technical Section of the Canadian Pulp and Paper Association, vol. 3 (5) 1979, pp. 66–73.
[23] S.P. Gaus, M.P. Harmer, H.M. Chan, H.S. Caram, N. Claussen, Alumina–alumide alloys (3a) technology: I, model development, J. Am. Ceram. Soc. 83 (2000) 1599–1605.
[24] D. de Faoite, D.J. Browne, K.T. Stanton, Regression analysis of temperature-dependent mechanical and thermal properties of dielectric technical ceramics, J. Mater. Sci. 48 (2013) 451–461.
[25] C. Dupont, R. Chiriac, G. Gauthier, F. Toche, Heat capacity measurements of various biomass types and pyrolysis residues, Fuel 115 (2014) 644–651.

[26] R.I. Coble, W.D. Kingery, Effect of porosity on physical properties of sintered alumina, J. Am. Ceram. Soc. 39 (1956) 377–385.
[27] M. Faessel, C. Delisée, F. Bos, P. Castéra, 3D modelling of random, cellulosic fibrous networks based on X-ray tomography and image analysis, Compos. Sci. Technol. 65 (2005) 1931–1940.
[28] C.T. Herakovich, S.C. Baxter, Influence of pore geometry on the effective response of porous media, J. Mater. Sci. 34 (1999) 1595–1609.
[29] C.A. Andersson, Derivation of the exponential relation for the effect of ellipsoidal porosity on elastic modulus, J. Am. Ceram. Soc. 79 (1996) 2181–2184.
[30] T. Isobe, T. Tomita, Y. Kameshima, A. Nakajima, K. Okada, Preparation and properties of porous alumina ceramics with oriented cylindrical pores produced by an extrusion method, J. Eur. Ceram. Soc. 26 (2006) 957–960.